CHEMISTRY
A EUROPEAN JOURNAL

DOI: 10.1002/chem.201000096

A General Approach to Fabricate Diverse Noble-Metal (Au, Pt, Ag, Pt/Au)/Fe_2O_3 Hybrid Nanomaterials

Jun Zhang, Xianghong Liu, Xianzhi Guo, Shihua Wu, and Shurong Wang*[a]

Abstract: A novel, facile, and general one-pot strategy is explored for the synthesis of diverse noble-metal (Au, Pt, Ag, or Pt/Au)/Fe_2O_3 hybrid nanoparticles with the assistance of lysine (which is a nontoxic, user friendly amino acid that is compatible with organisms) and without using any other functionalization reagents. Control experiments show that lysine, which contains both amino and carboxylic groups, plays dual and crucial roles as both linker and capping agents in attaching noble metals with a small size and uniform distribution onto an Fe_2O_3 support. Considering the perfect compatibility of lysine with organism, this approach may find potentials in biochemistry and biological applications. Furthermore, this novel route is also an attractive alternative and supplement to the current methods using a silane coupling agent or polyelectrolyte for preparing hybrid nanomaterials. To demonstrate the usage of such hybrid nanomaterials, a chemical gas sensor has been fabricated from the as-synthesized Au/Fe_2O_3 nanoparticles and investigated for ethanol detection. Results show that the hybrid sensor exhibits significantly improved sensor performances in terms of high sensitivity, low detection limit, better selectivity, and good reproducibility in comparison with pristine Fe_2O_3. Most importantly, this general approach can be further employed to fabricate other hybrid nanomaterials based on different support materials.

Keywords: amino acids · gold · iron oxides · nanoparticles · sensors

Introduction

In recent years, functional hybrid nanomaterials have attracted considerable research attention because a hybrid system that combines two or more compositions can usually provide novel or enhanced properties, which are not available from their individual components, for various applications in optics, magnetics, catalysts, medicine, chemical sensor, and biomedical applications.[1] Noble metals are known to have unique electronic and catalytic properties,[2] and can be further used to enhance the chemical and physical properties of functional nanomaterials. For instance, by constructing hybrid nanostructures, the magnetic, catalytic, cancer therapeutic, and plasmonic properties of metal oxides can be significantly improved.[1c,2a,3] More importantly, through controlling the loading amount of noble metals, the chemical or physical properties can be finely tuned and optimized.

[a] Dr. J. Zhang, Dr. X. Liu, Dr. X. Guo, Prof. S. Wu, Dr. S. Wang
Department of Chemistry, Nankai University
Tianjin, 300071 (China)
Fax: (+86) 22-2350-2458
E-mail: wsr618@gmail.com

To date, extensive progress has been obtained for the synthesis of hybrid nanomaterials. While there has been a large number of reports on such hybrid materials, the synthetic procedure has been limited and is still in great need for innovation. For example, by using a high-temperature (180 or 300 °C) thermal decomposition method, unique nanostructures such as dumbbell-like Au- and Pt-Fe_3O_4 or core-shell Fe_3O_4/Au nanoparticles have been synthesized.[1a,3b,4] Considering the ease of synthesis, fabrication cost, and potential for scaleup, a room-temperature, solution-based approach, especially when using water as the solvent, seems to be more advantageous. Guo et al.[5] have synthesized diverse noble-metal/Fe_3O_4, TiO_2, and carbon nanotube hybrids by using 3-aminopropyltrimethoxysilane (APTMS) as a linker, and found that the hybrid materials exhibited superior electrochemical properties. In addition, other linker reagents, such as poly(diallyldimethylammonium chloride),[6] 3-aminopropyltriethoxysilane,[7] $SnCl_2$,[8] and 1,6-hexadiamine[9] have also been explored to fabricate hybrid nanomaterials. For these synthetic approaches, two steps are usually required, including, first, functionalization of the support material surface with linker functional groups and, second, attachment of noble metals onto the functionalized material surface through interaction with the linker groups. Potentially these

synthetic processes can be further simplified to a facile one-pot synthesis by using nontoxic solvent and reagents, as demonstrated herein.

In this work, a more convenient one-pot procedure is explored for the synthesis of diverse noble-metal (Au, Pt, Ag, and Au/Pt)/Fe_2O_3 hybrid nanomaterials by using lysine as both a linker and protector for noble metals without additional functionalization of the support. Lysine, which has two kinds of functional groups ($-NH_2$ and $-COOH$), plays dual and crucial roles in attaching noble metals with a small size and uniform distribution onto Fe_2O_3 nanoparticles. In comparison with the above-mentioned functionalization reagents, such as silane coupling reagents or polyelectrolytes, lysine used in this work is cheap, nontoxic, environmentally benign, and user friendly. By using this novel and general method, diverse noble metals can be successfully loaded onto Fe_2O_3 nanoparticles to form hybrid nanomaterials, which should have great potential for applications such as biochemistry, magnetics, optics, catalysts, and sensors. For instance, we have fabricated a chemical gas sensor from the as-synthesized Au/Fe_2O_3 hybrid nanomaterials and investigated its gas-sensing properties by using ethanol as a probe molecule. Obtained results showed that the chemical sensor based on the Au/Fe_2O_3 hybrid material exhibited significantly enhanced sensing performance. It is further expected that this general method can be extended to produce other hybrid functional nanomaterials with enhanced properties or performances.

Results and Discussion

Peptides and proteins, due to their multifunctional groups, have recently become increasingly powerful in directing the synthesis of nanomaterials for various applications.[10] Lysine (an amino acid that serves as a basic building block for peptides) used in this work has a dual role as both linker and protecting reagents. In previous work by Sastry et al.,[11] lysine has been used as a capping reagent to stabilize small Au nanoparticles in aqueous solution. Subsequently, Zhong et al.[12] performed a systematic study on the interaction between amino acids and Au nanoparticles. They have also used the lysine-capped Au nanoparticles for preparing a CO oxidation catalyst.[13] Based on these pioneering works, we have further developed this lysine-assisted approach for fabricating hybrid materials.

Lysine has two kinds of functional groups, namely, NH_2 and COOH. The former is able to bind Au nanoparticles, thus making Au nanoparticles stable from aggregation and water dispersible.[11] Interestingly, powder-like lysine-capped Au nanoparticles can be obtained by evaporating the solvent, and can be redispersed in water,[11] which is highly attractive for use as nanobuiding blocks. In addition, both amino and carboxylic groups have been reported to be capable of coordinating with transition-metal ions in oxides,[14] thus implying that an amino acid can serve as a bridge or linker to anchor noble metals onto metal oxides to form hybrid Au/metal oxide nanomaterials. This approach is illustrated in Figure 1. The lysine-functionalized α-Fe_2O_3 nanoparticles can adsorb various noble metals due to the strong interactions between amino groups and metal particles.

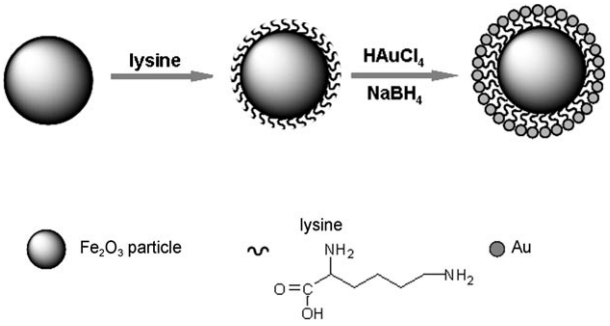

Figure 1. Schematic illustration of hybrid Au/Fe_2O_3 nanoparticle fabrication. The approach can also be extended to fabricate (Pt, Ag, and Pt/Au)/Fe_2O_3 hybrid nanomaterials by changing the noble-metal precursor.

α-Fe_2O_3, an n-type semiconductor widely used for catalyst, chemical sensor, and magnetic applications, has been selected as the support material to verify the effectiveness and feasibility of this novel approach. Figure 2 shows the

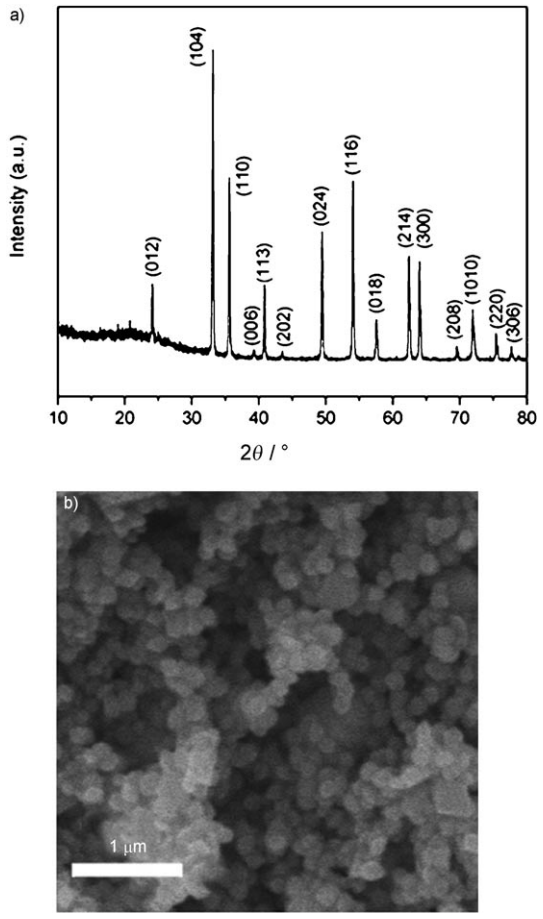

Figure 2. XRD spectrum (a) and SEM image (b) of the hydrothermally synthesized Fe_2O_3 nanoparticles.

XRD spectrum and SEM image of the synthesized Fe_2O_3 particles derived from a hydrothermal environment. The diffractions peaks of XRD (Figure 2a) agree perfectly with the indexation of the pure rhombohedral phase of α-Fe_2O_3 (JCPDS no. 33-0664). No impurity phase was detected by XRD analysis, indicating that the only crystallized hematite α-Fe_2O_3 was generated in the hydrothermal condition. From the SEM image (Figure 2b), it can be seen that the α-Fe_2O_3 has a pseudo sphere-like shape with a diameter of approximately 200 nm.

Figure 3a shows the TEM image of Au nanoparticles capped by lysine as a protecting agent. A high dispersion of Au nanoparticles with a small size can be observed from this picture. Interestingly, as indicated by the white squares in Figure 3a, some liner assemblies of Au nanoparticles can also be seen, which is a direct result of connection by the amino group of lysine,[12a,15] because each lysine molecule has two amino groups that can attach two Au nanoparticles. This phenomenon in turn confirms the strong interaction between amino groups and Au nanoparticles, which plays a crucial role in producing hybrid Au/Fe_2O_3 materials. Figure 3b displays the size histogram of Au nanoparticles, showing a narrow size distribution in the range of 3–8 nm with an average particle size of around 5.3 nm. Figure 3c shows the FTIR spectrum of lysine-functionalized Fe_2O_3 nanoparticles. The bands at 482 and 578 cm^{-1} correspond to Fe−O vibrations, whereas the bands at 3432 and 1635 cm^{-1} are ascribed to the N−H stretching from amino groups and C=O stretching from carboxylic groups;[5a,14d] this strongly confirms the adsorption of lysine on the surface of Fe_2O_3 nanoparticles. The amino groups on Fe_2O_3 nanoparticles are capable of adsorbing noble metals for constructing hybrid nanomaterials.

A group of TEM images of as-prepared Au/Fe_2O_3 hybrid nanoparticles are shown in Figure 4. From these images, it is observed that Au nanoparticle have been effectively immobilized onto Fe_2O_3 nanoparticles. In particular, in Figure 4b–d it can be seen that these small Au nanoparticles are uniformly distributed with a high density and a diameter in the range of 3–6 nm, irrespective of some individual large Au nanoparticles (as marked by an arrow in Figure 4b and c). The existence of large Au nanoparticles is probably due to aggregation of on initially small Au nanoparticles that act as seeds. To further confirm the formation of Au/Fe_2O_3 hybrid material, XPS analysis was performed. Figure 5 shows the high-resolution spectra of Fe 2p and Au 4f. In Figure 5a, the binding energy of Fe 2p at 710.5 and 723.8 eV confirms the oxidation state of Fe^{3+} in the hybrid material. The Au 4f spectrum (Figure 5b) shows two binding energies at 83.6 and 87.2 eV, corresponding to the metallic state of Au. In addition, the XPS test reveals that the Au loading content in the hybrid material is 6.83 wt%.

To support the efficient and important role of lysine in the synthesis of hybrid materials, a control experiment is conducted in the absence of lysine, while keeping other parameters unchanged. The TEM images of as-synthesized Au/Fe_2O_3 without using lysine are displayed in Figure 6. In comparison with Figure 4, it can be seen clearly that the Au nanoparticles show a poor distribution on the Fe_2O_3 support surface. Many Fe_2O_3 nanoparticles still remain a smooth surface, rather than the rough surface of the Au-decorated Fe_2O_3 nanoparticles, as shown in Figure 4. This clearly confirms the significant role of lysine in attaching Au nanoparticles onto Fe_2O_3 nanoparticles. Furthermore, in Figure 6c and d, the Au nanoparticles also possess a rather poor size distribution from several to twenty nanometers, which is due to the lack of capping by lysine.

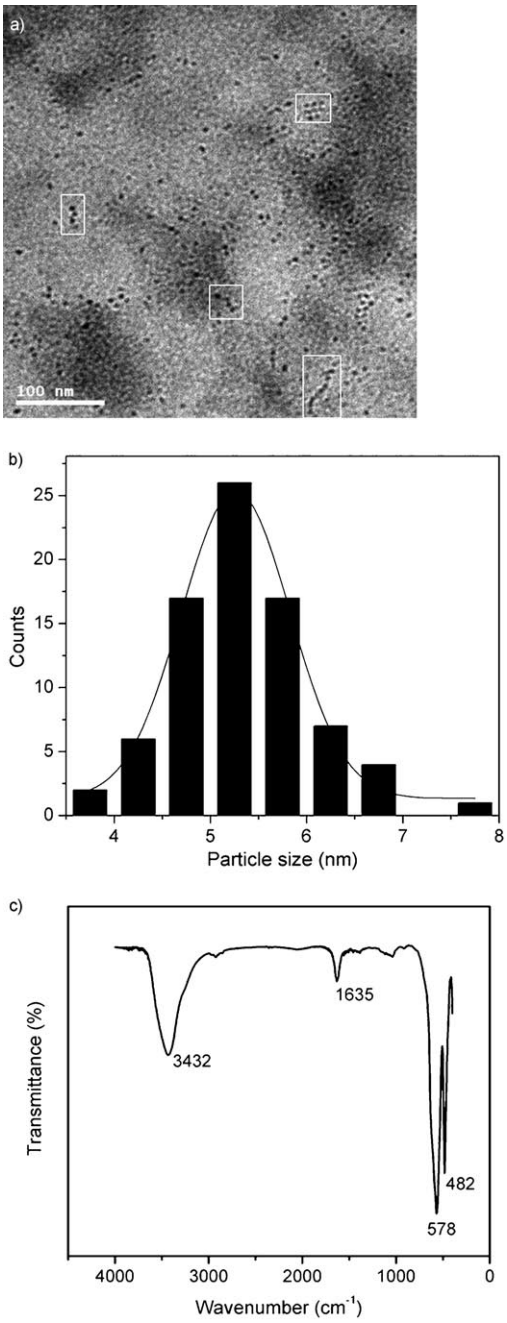

Figure 3. a) TEM image and b) size distribution histogram of Au nanoparticles capped by lysine, and c) FTIR spectrum of lysine-functionalized Fe_2O_3 nanoparticles.

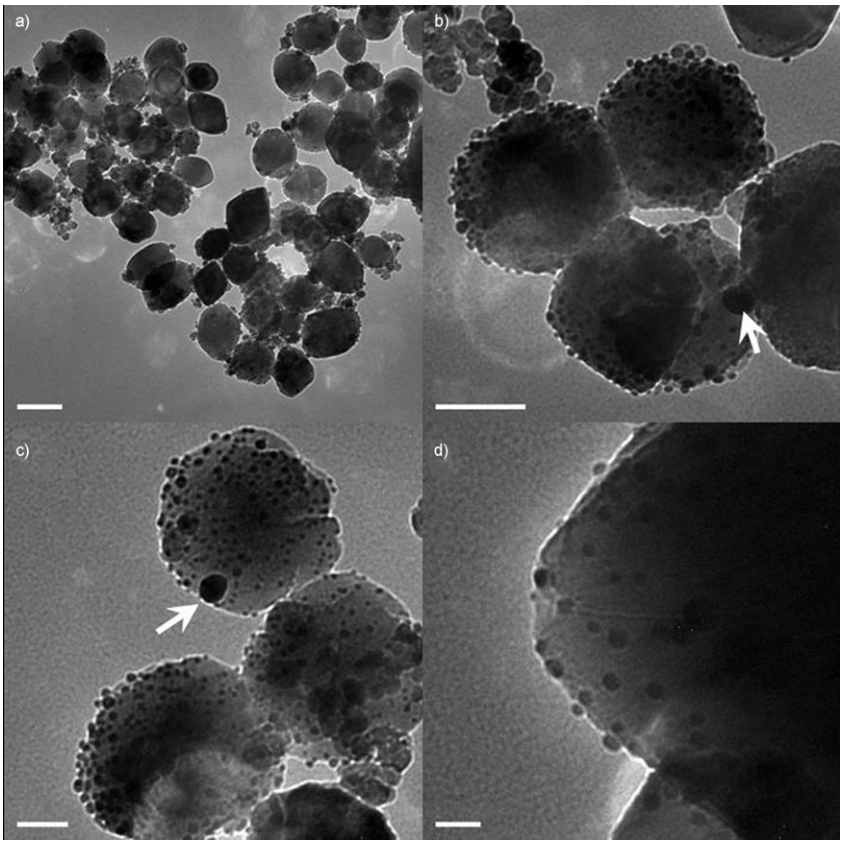

Figure 4. TEM images of hybrid Au/Fe_2O_3 nanoparticles with different magnifications (scale bars: 0.2 μm (a), 100 nm (b), 50 nm (c), and 20 nm (d)) synthesized in the presence of lysine.

Nowadays, a general method for fabricating hybrid nanomaterials is highly attractive and is of great significance from both scientific and applicable perspectives. To elucidate the generality of this lysine-assisted approach, we have attempted to synthesize Pt and Ag hybrid nanoparticles by using this method. TEM images of the prepared Pt/Fe_2O_3 and Ag/Fe_2O_3 hybrid nanoparticles are exhibited in Figures 7 and 8, respectively. Figure 7a–c shows that Pt/Fe_2O_3 hybrids have been successfully fabricated by this lysine-assisted method. The Pt nanoparticles also exhibit a highly uniform dispersion and small sizes of only several nanometers, which is even smaller than that of the Au nanoparticles shown in Figure 4c and d. Figure 7d shows the XPS pattern of Pt 4f, which has two binding energies located at 71.2 and 74.4 eV, which can be ascribed to metallic Pt. The loading amount of Pt nanoparticles in the Pt/Fe_2O_3 hybrid material detected by XPS is 14.17 wt%. We further extend this method to synthesize Ag/Fe_2O_3 hybrid nanoparticles. The representative TEM images are exhibited in Figure 8a and b. It can be seen that the loading density of Ag nanoparticles are not as high as those of Au/Fe_2O_3 and Pt/Fe_2O_3 hybrids. Furthermore, these Ag nanoparticles have a relatively large size of approximately 20 nm. Figure 8c demonstrates the XPS spectrum of Ag 3d, showing two binding energies at 367.6 and 373.3 eV. The Ag loading amount determined by XPS is only 2.86 wt%.

To date, multicomponent hybrid materials have received considerable research attention due to the synergism interaction between their compositions, which should have superior properties to their individual counterparts. Very recently, multicomponent nanomaterials composed of binary noble metals have become a hot topic in the area of materials science and is currently receiving growing interest. For example, Guo et al.[16] have synthesized hybrid Au/Pt nanoparticles with much higher catalytic activity for the oxygen reduction reaction. In addition, by using APTMS as a linker, they have also successfully attached hybrid Au/Pt and Au/Ag nanoparticles onto diverse support materials.[5a] An

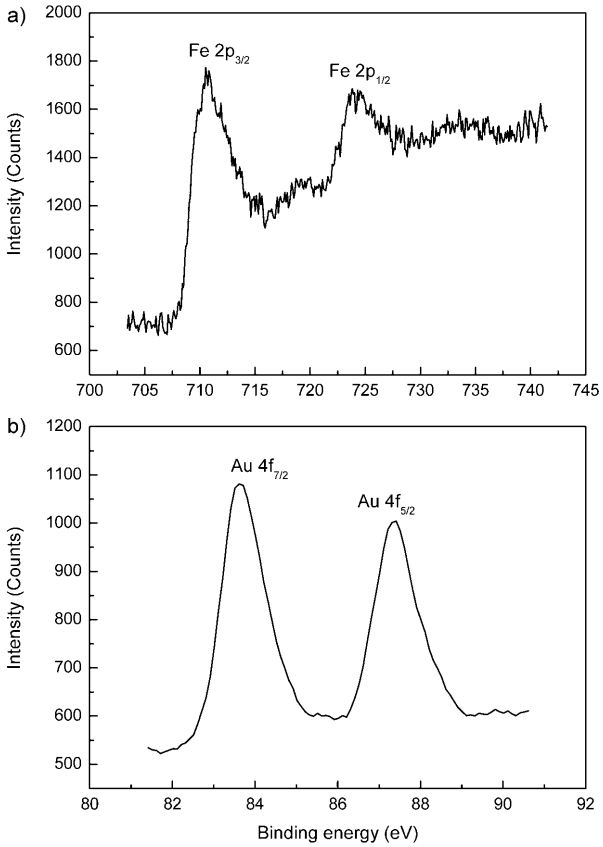

Figure 5. XPS spectra of Fe 2p (a) and Au 4f (b) of hybrid Au/Fe_2O_3 nanoparticles.

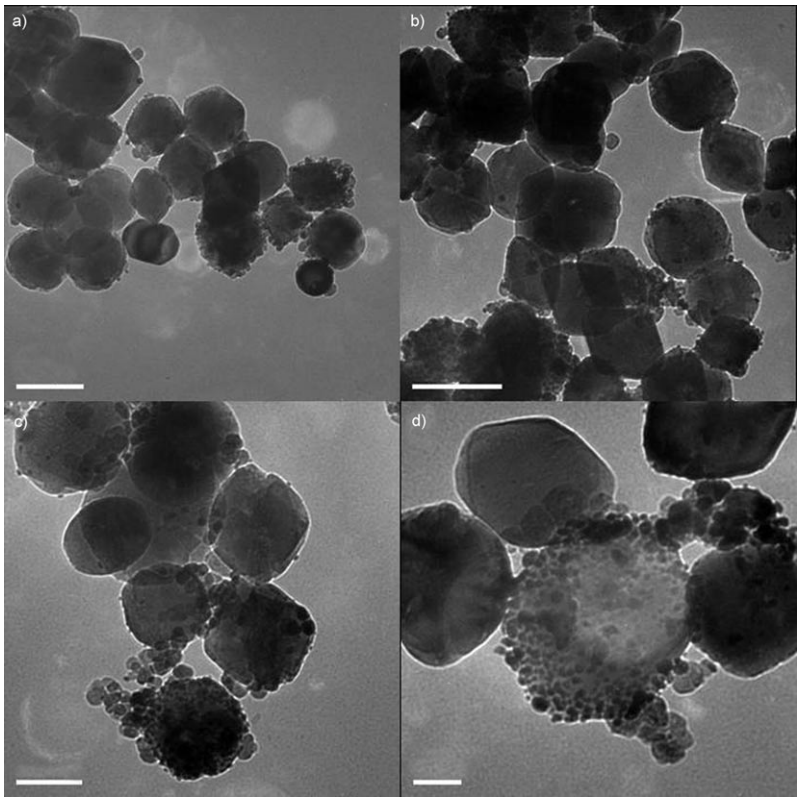

Figure 6. TEM images of hybrid Au/Fe_2O_3 nanoparticles with different magnifications (scale bars: 0.2 μm (a), 200 nm (b), 100 nm (c), and 50 nm (d)) synthesized in the absence of lysine.

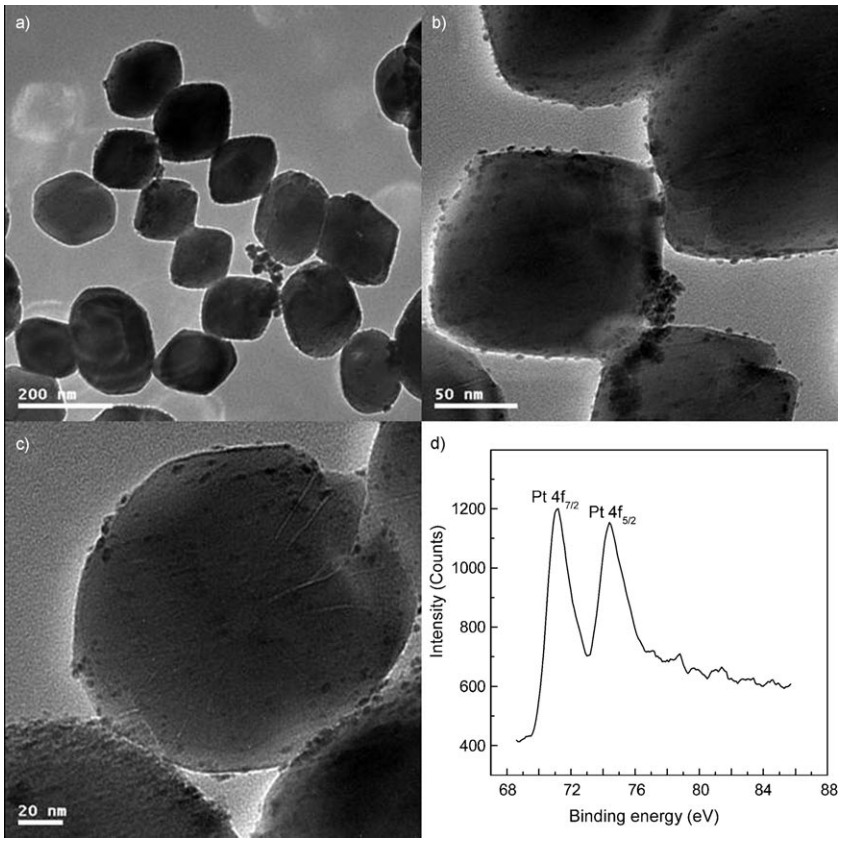

Figure 7. TEM images (a–c) and XPS spectrum (d) of Pt 4f of the Pt/Fe_2O_3 hybrid nanoparticles.

interesting hybrid Au/Pt hollow nanospheres has been reported by Liang and co-workers[17] by using Co nanoparticles as sacrificial templates. Another example is Au/Pt alloy nanoparticles fabricated by Lou et al.[18] for applications in methanol oxidation. It should be pointed out that the idea of hybridization of noble metals has provided researchers a powerful means to explore or tune the chemical or physical properties of nanomaterials, thus enlarging their applications in magnetics, electrocatalyst, optics, and so forth. Herein, we have also fabricated ternary $Pt/Au/Fe_2O_3$ hybrid nanoparticles by using preformed Au/Fe_2O_3 nanoparticles as the support. The images are given in Figure 9a and b. In comparison to the Au/Fe_2O_3 nanoparticles in Figure 4a–d, no significant difference is observed. However, XPS analysis clearly confirms that Pt has been successfully supported on the preformed Au/Fe_2O_3 nanoparticles. High-resolution XPS spectra of Au 4f and Pt 4f are illustrated in Figure 9c and d, showing their respective binding energies at 83.7 and 87.3 eV for Au and 71.3 and 74.5 eV for Pt. Interestingly, it is found that the binding energies of Au 4f and Pt 4f in this ternary hybrid system exhibit a positive shift in comparison with the above-synthesized binary nanoparticles. A similar result has been reported for Co/Pt hybrid hollow spheres by Chen and coworkers.[19] Additionally, the chemical environment (for instance, different support materials) of noble metals also has a significant influence on their binding energies.[4c,20] XPS analyses also reveal that the loading of Pt and Au is 5.06 and 5.55 wt%, respectively. Note that the detected Au content (5.55 wt%) is lower than that (6.83 wt%) of preformed Au/Fe_2O_3 nano-

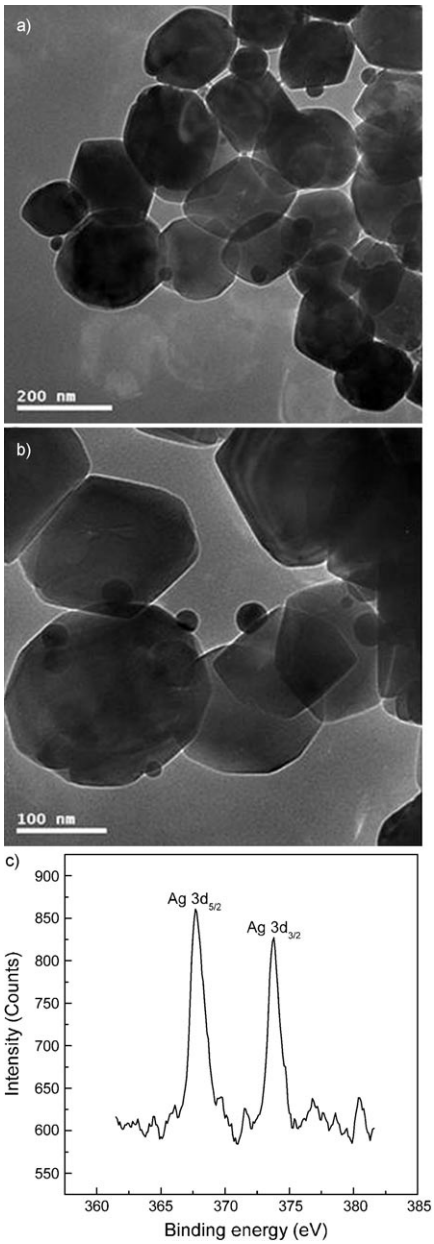

Figure 8. TEM images (a, b) and XPS spectrum of Ag 3d (c) of Ag/Fe_2O_3 hybrid nanoparticles.

particles. This is probably due to Au nanoparticles acting as seeds for the growth of Pt nanoparticles[16] and thus is covered by the Pt composition. On the other hand, this result is also a strong support for the successful attachment of Pt onto Au/Fe_2O_3 nanoparticles in the presence of lysine.

Noble metals, take Au nanoparticles for example, are highly commended for catalyzing various reactions, such as hydrochlorination, low-temperature CO oxidation, and selective alcohol oxidation, due to unique catalytic and electronic activities.[4,21] Nowadays, there is growing interest in employing noble metals as a promoter for enhancing the performances of chemical sensors,[22] due to the synergic interaction between noble metals and oxide supports, which may play an important role in improving the chemical properties of materials.[23] Herein, we have fabricated a chemical gas sensor from the prepared hybrid Au/Fe_2O_3 nanoparticles and ethanol is tested as a probe molecule to examine the sensor properties. For comparison, a chemical sensor based on pristine Fe_2O_3 nanoparticles is also fabricated. For chemical resistive gas sensors, it is known that the test gas concentration has a large influence on the sensor response. The concentration-dependent sensor response behavior was examined by exposure to 5, 50, 200, and 500 ppm ethanol. Figure 10 shows the dynamic response-recovery curves of the two sensors to different ethanol concentrations. It can be seen that the Au/Fe_2O_3 sensor is much more sensitive than the pristine one. The response amplitude of the Au/Fe_2O_3 sensor is significantly increased with increasing ethanol concentration, while the increase in the response of the pristine one is almost negligible. Sensitivity is another important factor of chemical sensors, a higher sensitivity can usually allow for a lower detection limit. Numerous efforts have been made to improve the sensor sensitivity and detection limit, in which the strategy of introducing noble metals into sensor matrix materials has proven to be very effective. In Figure 10, take 5 ppm ethanol for example, the pristine Fe_2O_3 sensor only gives a negligible response, whereas the response of the Au/Fe_2O_3 sensor is significantly enhanced, which in turn directly verifies the promotion effect of Au nanoparticles. Reasonably, the detection limit for ethanol can be down to the ppm level. The sensor sensitivities to different ethanol concentrations are compared in Figure 11, showing that the Au/Fe_2O_3 sensor has much higher sensitivities. On exposure to 5 ppm ethanol, the sensitivity for Au/Fe_2O_3 sensor is 6.08, which is nearly four times higher than that (1.66) of the pristine one. As show in Figure 11, with increasing gas concentration, the sensor sensitivity is further improved due to the hybridization of Au nanoparticles. Sensor sensitivities to three other gases have been tested and compared to demonstrate the selectivity of the sensors. The result is displayed in Figure 12. Clearly, the sensitivities of the Au/Fe_2O_3 sensor to four gases are all improved to some extent, however, the largest increase in sensor sensitivity is only observed for ethanol, implying the good sensor selectivity for alcohol. Stability, that is, the ability to successively respond to a target gas without a visible decrease in sensor response, is another important feature of chemical sensor. Figure 13 illustrates the reproducibility of the Au/Fe_2O_3 sensor, revealing that the sensor maintains its initial response amplitude without a clear decrease upon three successive sensing tests to 100 ppm ethanol.

Conclusion

A facile, efficient, and general one-pot method was successfully developed for fabricating diverse noble-metal (Au, Pt, Ag, and Pt/Au)/Fe_2O_3 hybrid nanomaterials. An environmentally benign and user friendly reagent, lysine, was used to load diverse noble metals onto Fe_2O_3 nanoparticles.

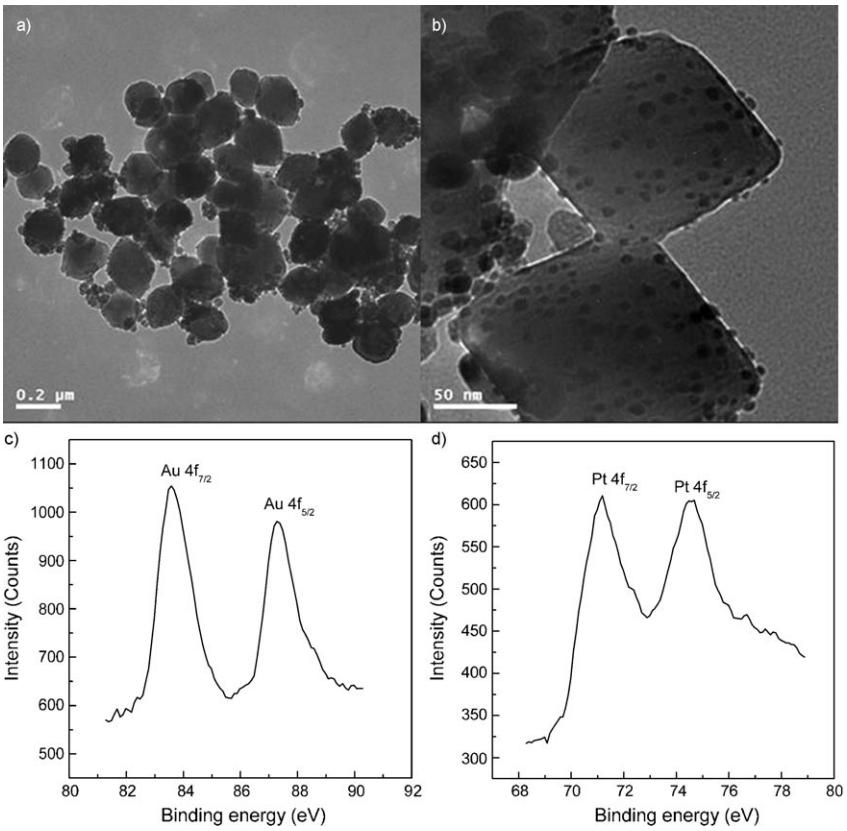

Figure 9. TEM images (a, b) and XPS spectra of Au 4f (c) and Pt 4f (d) of ternary $Pt/Au/Fe_2O_3$ hybrid nanoparticles.

nanoparticles. For synthesis, only lysine with its dual role is used and no other functionalization reagents are needed. A multicomponent hybrid nanomaterial, such as $Pt/Au/Fe_2O_3$, can also be produced by this approach. 2) Lysine, an essential amino acid for the human body, is nontoxic, low cost, and particularly important in biochemistry. Its perfect compatibility with organisms may provide lysine-capped Au nanoparticles with the potential to act as powerful nanobuilding blocks in biological applications. 3) The as-prepared noble-metal/Fe_2O_3 hybrid nanomaterials, $Au//Fe_2O_3$ nanoparticles, for example, have shown significantly improved sensor performances in terms of high sensitivity, ppm level detection limits, better selectivity, and good reproducibility. 4) Most importantly, this synthetic strategy is general and can be employed to fabricate other hybrid nanomaterials based on different support materials with either rod-like, hollow, or hierarchical nanostructures, and progress in this direction is underway.

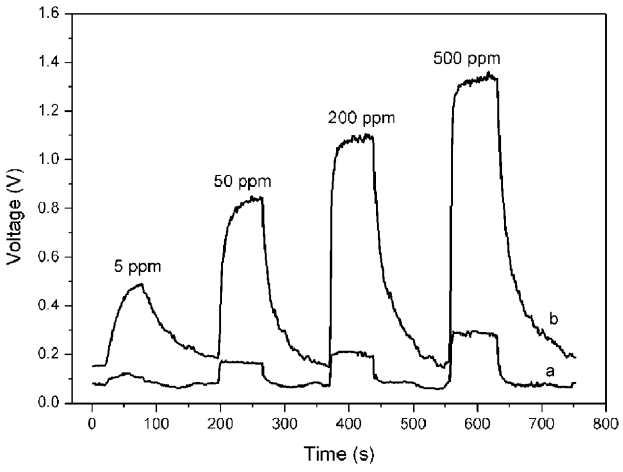

Figure 10. Dynamic response-recovery curves of the two sensors (pristine Fe_2O_3 (a) and Au/Fe_2O_3 (b)) to different ethanol concentrations.

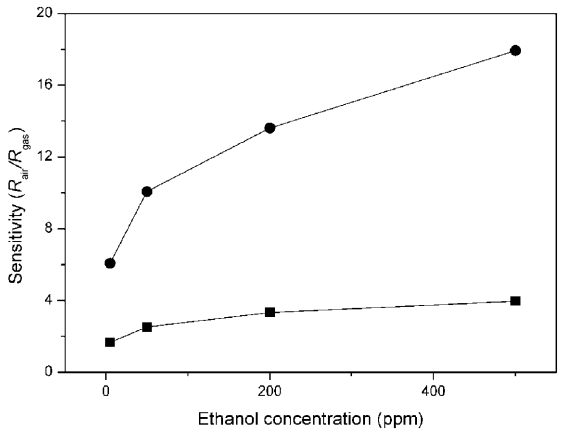

Figure 11. Comparison in sensor sensitivities to different ethanol concentrations for Fe_2O_3 (■) and Au/Fe_2O_3 (●).

Lysine used in this work has a dual role of both a linker to attach noble metals to the Fe_2O_3 matrix and a capping reagent to stabilize small Au nanoparticles with uniform dispersion. This method has the following advantages: 1) The synthesis is a facile one-pot method, in which the noble metals are formed and simultaneously supported on Fe_2O_3

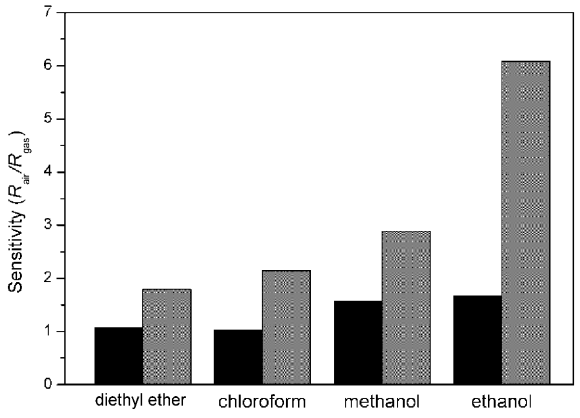

Figure 12. Comparison in sensor sensitivities to different gases with a same concentration for Fe_2O_3 (black) and Au/Fe_2O_3 (gray) of 5 ppm.

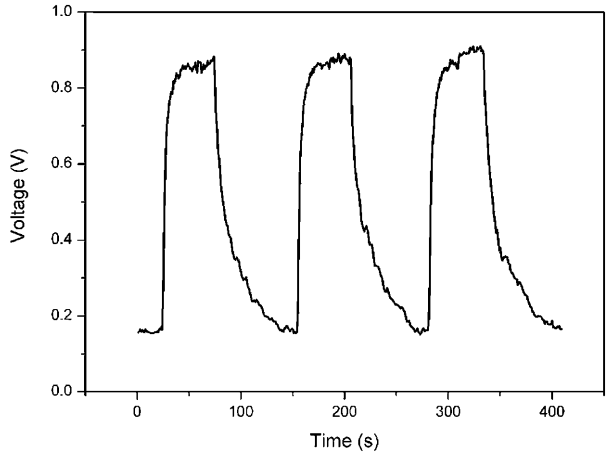

Figure 13. Reproducibility of the Au/Fe_2O_3 sensor on successive exposure (3 cycles) to 100 ppm ethanol.

Experimental Section

Materials: Chemicals such as $FeCl_3 \cdot 6H_2O$, ethanol, lysine, and $NaBH_4$ were of analytical grade and purchased from Guangfu Fine Chemical Research Institute (Tianjin, China). $HAuCl_4 \cdot 4H_2O$, $H_2PtCl_6 \cdot 6H_2O$, $AgNO_3$ were obtained from Yingdaxigui Chemical Reagent Company (Tianjin, China). Distilled water was used throughout the experiments.

Synthesis of Fe_2O_3 nanoparticles: Fe_2O_3 nanoparticles were prepared by a hydrothermal process. In a typical synthesis, a 0.02 M aqueous solution of $FeCl_3$ was sealed in Teflon-lined autoclaves with a fill volume of 80% and kept at 100 °C for 3 d. After reaction, the autoclaves were cooled to room temperature naturally. The red precipitate was centrifuged and washed with distilled water and ethanol several times, then dried at 80 °C for several hours.

Lysine-capped Au nanoparticles: The synthesis of Lysine-capped Au nanoparticles followed the literature method[11] with minor modifications. First, a 0.01 M aqueous solution of $HAuCl_4$ (0.5 mL) together with a 0.01 M aqueous solution of lysine (0.5 mL) was diluted to 50 mL with distilled water. Then $NaBH_4$ (0.005 g) was added into the above solution. Within a few seconds, the color of the solution turned from light yellow to ruby red, indicating the formation of small Au nanoparticles.

Synthesis of Au/Fe_2O_3 hybrid nanoparticles: As-prepared Fe_2O_3 nanoparticles (0.8 g) were dispersed into water (10 mL) under stirring, followed by adding a 0.01 M aqueous solution of lysine (16 mL) and a 0.01 M aqueous solution of $HAuCl_4$ (10 mL). After sonication for 30 min, a 0.1 M aqueous solution of $NaBH_4$ (10 mL) was added into the reaction system. The reaction was maintained for 2 h and then centrifuged and washed with water and ethanol several times. The Au/Fe_2O_3 hybrid material obtained was dried at 80 °C.

Synthesis of Pt/Fe_2O_3 hybrid nanoparticles: Fe_2O_3 nanoparticles (0.4 g) were dispersed into water (10 mL) under stirring, followed by adding a 0.01 M aqueous solution of lysine (10 mL) and a 0.0077 M aqueous solution of H_2PtCl_6 (5 mL). After sonication for 30 min, a 0.1 M aqueous solution of $NaBH_4$ (5 mL) was added into the reaction system. The reaction was maintained for 2 h and then centrifuged and washed with water and ethanol several times. The obtained Pt/Fe_2O_3 hybrid material was dried at 80 °C.

Synthesis of Ag/Fe_2O_3 hybrid nanoparticles: Fe_2O_3 nanoparticles (0.4 g) were dispersed into water (10 mL) under stirring, followed by adding a 0.01 M aqueous solution of lysine (10 mL) and a 0.01 M aqueous solution of $AgNO_3$ (5 mL). After sonication for 30 min, a 0.1 M aqueous solution of $NaBH_4$ (5 mL) was added into the reaction system. The reaction was maintained for 2 h and then centrifuged and washed with water and ethanol several times. The obtained Ag/Fe_2O_3 hybrid material was dried at 80 °C.

Synthesis of ternary $Pt/Au/Fe_2O_3$ hybrid nanoparticles: As-prepared Au/Fe_2O_3 hybrid nanoparticles (0.4 g) were dispersed into water (10 mL) under stirring, followed by adding a 0.01 M aqueous solution of lysine (6 mL) and a 0.0077 M aqueous solution of H_2PtCl_6 (2 mL). After sonication for 30 min, a 0.1 M aqueous solution of $NaBH_4$ (2 mL) was added into the reaction system. The reaction was kept for 2 h and then centrifuged and washed with water and ethanol several times. The obtained $Pt/Au/Fe_2O_3$ hybrid material was dried at 80 °C.

Characterization: Prior to characterization, all of the materials were heated at 300 °C for 1 h to remove organic lysine. The phase composition and morphology of samples were characterized by XRD analysis (Rigaku D/max-2500, graphite monochromator, $Cu_{K\alpha}$, $\lambda = 1.5418$ Å), SEM (Shimadzu SS-550, 15 kV), TEM (Philips FEI Tecnai 20ST, 200 kV), and XPS (Kratos Axis Ultra DLD spectrometer, $Al_{K\alpha}$ X-ray monochromator). Gas-sensing properties of the hybrid material were tested on a commercial HW-30A gas-sensing measurement system (HanWei Electronics Co., Ltd., Henan, China) at an operating temperature of 320 °C and a relative humidity of 18–30%. Details of the sensor fabrication and test can be seen in our previous works.[24] A calculated amount of the target ethanol was introduced into the test chamber on the HW-30A instrument by a microsyringe. The sensor sensitivity is defined as the ratio of R_{air}/R_{gas}, in which R_{air} and R_{gas} are the electrical resistance of the sensor in air and in test gas, respectively.

Acknowledgements

This work was supported by the National Natural Science Foundation of China (no. 20871071) and the Applied Basic Research Programs of Science and Technology Commission Foundation of Tianjin (nos. 08JCYBJC00100 and 09JCYBJC03600).

[1] a) E. V. Shevchenko, M. I. Bodnarchuk, M. V. Kovalenko, D. V. Talapin, R. K. Smith, S. Aloni, W. Heiss, A. P. Alivisatos, *Adv. Mater.* **2008**, *20*, 4323; b) G. Lu, L. E. Ocola, J. C. G. Kwon, Y. Jang, M.-h. Park, J. Moon, J. S. Son, I. C. Song, W. K. Moon, T. Hyehen, *Adv. Mater.* **2009**, *21*, 2487; c) S.-H. Choi, H. B. Na, Y. I. Park, K. An, Son, *J. Am. Chem. Soc.* **2008**, *130*, 15573; d) H. W. Gu, P. L. Ho, K. W. T. Tsang, L. Wang, B. Xu, *J. Am. Chem. Soc.* **2003**, *125*, 15702; e) S. T. Selvan, P. K. Patra, C. Y. Ang, J. Y. Ying, *Angew. Chem.* **2007**, *119*, 2500; *Angew. Chem. Int. Ed.* **2007**, *46*, 2448; f) D. K. Yi, S. T. Selvan, S. S. Lee, G. C. Papaefthymiou, D. Kundaliya, J. Y. Ying, *J. Am. Chem. Soc.* **2005**, *127*, 4990.

[2] a) A. S. K. Hashmi, G. J. Hutchings, *Angew. Chem.* **2006**, *118*, 8064; *Angew. Chem. Int. Ed.* **2006**, *45*, 7896; b) M. C. Daniel, D. Astruc, *Chem. Rev.* **2004**, *104*, 293.

[3] a) Z. Xu, Y. Hou, S. Sun, *J. Am. Chem. Soc.* **2007**, *129*, 8698; b) W. L. Shi, H. Zeng, Y. Sahoo, T. Y. Ohulchanskyy, Y. Ding, Z. L. Wang, M. Swihart, P. N. Prasad, *Nano Lett.* **2006**, *6*, 875.
[4] a) C. Xu, B. Wang, S. Sun, *J. Am. Chem. Soc.* **2009**, *131*, 4216; b) H. Yu, M. Chen, P. M. Rice, S. X. Wang, R. L. White, S. Sun, *Nano Lett.* **2005**, *5*, 379; c) C. Wang, H. Daimon, S. Sun, *Nano Lett.* **2009**, *9*, 1493.
[5] a) S. Guo, S. Dong, E. Wang, *Chem. Eur. J.* **2009**, *15*, 2416; b) S. Guo, S. Dong, E. Wang, *J. Phys. Chem. C* **2008**, *112*, 2389; c) S. Guo, J. Li, E. Wang, *Chem. Asian J.* **2008**, *3*, 1544.
[6] S. Wang, S. P. Jiang, T. J. White, J. Guo, X. Wang, *Adv. Funct. Mater.* **2009**, *19*, 1.
[7] X. Liu, A. Wang, X. Yang, T. Zhang, C.-Y. Mou, D.-S. Su, J. Li, *Chem. Mater.* **2009**, *21*, 410.
[8] L.-S. Zhong, J.-S. Hu, Z.-M. Cui, L.-J. Wan, W.-G. Song, *Chem. Mater.* **2007**, *19*, 4557.
[9] J. Bao, W. Chen, T. Liu, Y. Zhu, P. Jin, L. Wang, J. Liu, Y. Wei, Y. Li, *ACS Nano* **2007**, *1*, 293.
[10] a) H. Heinz, B. L. Farmer, R. B. Pandey, J. M. Slocik, S. S. Patnaik, R. Pachter, R. R. Naik, *J. Am. Chem. Soc.* **2009**, *131*, 9704; b) M. B. Dickerson, K. H. Sandhage, R. R. Naik, *Chem. Rev.* **2008**, *108*, 4935; c) W. Jiang, S. Mardyani, H. Fischer, W. C. W. Chan, *Chem. Mater.* **2006**, *18*, 872; d) J. Malicka, I. Gryczynski, W. Jiang, H. Fischer, W. C. W. Chan, Z. Gryczynski, W. Grudzinski, J. R. Lakowicz, *J. Phys. Chem. B* **2005**, *109*, 1088.
[11] P. Selvakannan, S. Mandal, S. Phadtare, R. Pasricha, M. Sastry, *Langmuir* **2003**, *19*, 3545.
[12] a) Z. Zhong, J. Luo, T. P. Ang, J. Highfield, J. Lin, A. Gedanken, *J. Phys. Chem. B* **2004**, *108*, 18119; b) Z. Zhong, S. Patskovskyy, P. Bouvrette, J. H. T. Luong, A. Gedanken, *J. Phys. Chem. B* **2004**, *108*, 4046.
[13] a) Z. Zhong, J. Ho, J. Teo, S. Shen, A. Gedanken, *Chem. Mater.* **2007**, *19*, 4776; b) Z. Zhong, J. Lin, S.-P. Teh, J. Teo, F. M. Dautzenberg, *Adv. Funct. Mater.* **2007**, *17*, 1402.
[14] a) O. Durupthy, J. Bill, F. Aldinger, *Cryst. Growth Des.* **2007**, *7*, 2696; b) J. Bandara, K. Tennakone, J. Kiwi, *Langmuir* **2001**, *17*, 3964; c) J. Zhu, O. K. Tan, Y. C. Lee, T. S. Zhang, B. Y. Tay, J. Ma, *Nanotechnology* **2006**, *17*, 5960; d) J. Y. Park, E. S. Choi, M. J. Baek, G. H. Lee, *Mater. Lett.* **2009**, *63*, 379.
[15] Q. Dai, J. G. Worden, J. Trullinger, Q. Huo, *J. Am. Chem. Soc.* **2005**, *127*, 8008.
[16] S. Guo, S. Dong, E. Wang, *J. Phys. Chem. C* **2009**, *113*, 5485.
[17] H.-P. Liang, Y.-G. Guo, H.-M. Zhang, J.-S. Hu, L.-J. Wan, C.-L. Bai, *Chem. Commun.* **2004**, 146.
[18] Y. Lou, M. M. Maye, L. Han, J. Luo, C.-J. Zhong, *Chem. Commun.* **2001**, 473.
[19] G. Chen, D. Xia, Z. Nie, Z. Wang, L. Wang, L. Zhang, J. Zhang, *Chem. Mater.* **2007**, *19*, 1840.
[20] a) Y. Xie, K. Ding, Z. Liu, R. Tao, Z. Sun, H. Zhang, G. An, *J. Am. Chem. Soc.* **2009**, *131*, 6648; b) K. Yu, Z. C. Wu, Q. R. Zhao, B. X. Li, Y. Xie, *J. Phys. Chem. C* **2008**, *112*, 2244.
[21] C. Della Pina, E. Falletta, L. Prati, M. Rossi, *Chem. Soc. Rev.* **2008**, *37*, 2077.
[22] N. Yamazoe, *Sens. Actuators B* **1991**, *5*, 7.
[23] Q. Fu, T. Wagner, *Surf. Sci. Rep.* **2007**, *62*, 431.
[24] a) J. Zhang, S. Wang, M. Xu, Y. Wang, B. Zhu, S. Zhang, W. Huang, S. Wu, *Cryst. Growth Des.* **2009**, *9*, 3532; b) J. Zhang, S. Wang, Y. Wang, Y. Wang, B. Zhu, H. Xia, X. Guo, S. Zhang, W. Huang, S. Wu, *Sens. Actuators B* **2009**, *135*, 610; c) J. Zhang, S. Wang, Y. Wang, M. Xu, H. Xia, S. Zhang, W. Huang, X. Guo, S. Wu, *Sens. Actuators B* **2009**, *139*, 411.

Received: January 14, 2010
Published online: June 11, 2010

